REPORT DOCUMENTATION PAGE

Form Approved
OMB No. 0704-0188

PLEASE DO NOT RETURN YOUR FORM TO THE ABOVE ORGANIZATION.

1. REPORT DATE *(DD-MM-YYYY)*	2. REPORT TYPE	3. DATES COVERED *(From - To)*
28/05/2012	Final Report	01/08/2009 - 14/02/2012

4. TITLE AND SUBTITLE
A GENERALIZED FINITE ELEMENT METHOD FOR MULTISCALE SIMULATIONS

5a. CONTRACT NUMBER
FA9550-09-1-0401

5b. GRANT NUMBER
FA9550-09-1-0401

5c. PROGRAM ELEMENT NUMBER

6. AUTHOR(S)
Carlos Armando Duarte

5d. PROJECT NUMBER

5e. TASK NUMBER

5f. WORK UNIT NUMBER

7. PERFORMING ORGANIZATION NAME(S) AND ADDRESS(ES)
University of Illinois at Urbana-Champaign
2122 Newmark Lab., MC-250
205 N. Mathews Av.
Urbana, IL 61801

8. PERFORMING ORGANIZATION REPORT NUMBER

9. SPONSORING/MONITORING AGENCY NAME(S) AND ADDRESS(ES)
Air Force Office of Science and Research
875 Randolph Street
Suite 325 Room 3112
Arlington, VA 22203

10. SPONSOR/MONITOR'S ACRONYM(S)
AFOSR

11. SPONSOR/MONITOR'S REPORT NUMBER(S)
AFRL-OSR-VA-TR-2012-1030

12. DISTRIBUTION/AVAILABILITY STATEMENT
Approved for Public Release

13. SUPPLEMENTARY NOTES

14. ABSTRACT

This report focuses on recent advances of the Generalized Finite Element Method (GFEM) for multiscale simulations. This method is based on the solution of interdependent global and local scale problems, and can be applied to a broad class of multiscale problems of relevance to the United States Air Force. The local problems focus on the resolution of fine scale features of the solution while the global problem addresses the macro-scale structural behavior. The local solutions are embedded into the global solution space using the partition of unity method.
A rigorous a-priori error estimate for the method is presented along with numerical verification of convergence properties predicted by the estimate. The convergence analysis shows optimal convergence of the method on problems with strong singularities. It also shows that the method can deliver the same accuracy as direct numerical simulations (DNS) while using meshes with elements that are orders of magnitude larger than in the DNS case.

15. SUBJECT TERMS
Computational Mathematics, Computational Methods, Finite Elements, Multiscale, Error Estimates.

16. SECURITY CLASSIFICATION OF:			17. LIMITATION OF ABSTRACT	18. NUMBER OF PAGES	19a. NAME OF RESPONSIBLE PERSON
a. REPORT	b. ABSTRACT	c. THIS PAGE			Carlos Armando Duarte
U	U	U	UU	18	19b. TELEPHONE NUMBER *(Include area code)* 217-417-0571

A GENERALIZED FINITE ELEMENT METHOD FOR
MULTISCALE SIMULATIONS

FA9550-09-1-0401

C. Armando Duarte
Dept. of Civil and Environmental Engineering
Computational Science and Engineering Program
University of Illinois at Urbana-Champaign

Abstract

This report focuses on recent advances of the Generalized Finite Element Method (GFEM) for multiscale simulations. This method is based on the solution of interdependent global and local scale problems, and can be applied to a broad class of multiscale problems of relevance to the United States Air Force. The local problems focus on the resolution of fine scale features of the solution while the global problem addresses the macro-scale structural behavior. The local solutions are embedded into the global solution space using the partition of unity method.

A rigorous *a-priori* error estimate for the method is presented along with numerical verification of convergence properties predicted by the estimate. The convergence analysis shows optimal convergence of the method on problems with strong singularities. It also shows that the method can deliver the same accuracy as direct numerical simulations (DNS) while using meshes with elements that are orders of magnitude larger than in the DNS case.

Recent advances of the GFEM for three-dimensional propagating fractures are also presented. The GFEM enables accurate simulations of this class of problems using finite element meshes with elements that are orders of magnitude larger than those required by the FEM. The intrinsic parallelism of the enrichment function computations is also explored in this research. The parallel efficiency of the method on a shared memory multi-processor machine is demonstrated on a three-dimensional problem with complex geometry.

This document further reports on extensions of the method to multiscale problems exhibiting nonlinear behavior. The nonlinear model problem focuses on structures with plastic deformations at regions that are orders of magnitude smaller than the dimensions of the structural component. It is shown that the multiscale GFEM can produce accurate nonlinear solutions at a reduced computational cost compared with available FEMs.

We conclude with some novel results on the Stable GFEM. The enrichment functions in this method are modified in order to further reduce discretization error without increasing the problem size. It is shown that the Stable GFEM also leads to significant improvements on the numerical conditioning of the method at a negligible computational cost.

Bridging Scales with Global-Local Enrichment Functions

Generalized FEM approximation spaces (i.e., trial spaces) consist of three components – (a) patches or clouds, (b) a partition of unity, and (c) the patch or cloud approximation spaces.

The Generalized Finite Element method with global-local enrichments ($GFEM^{\mathrm{gl}}$) combines the classical global-local finite element method with the partition of unity approach. In contrast to the standard Generalized/eXtended FEMs, which use analytical enrichment functions, this method provides a framework to enrich the solution space with functions obtained from the solution of a local boundary value problem. The boundary conditions for this problem are obtained from the solution of the global problem discretized with a coarse finite element mesh. The local problems can be accurately solved using the *hp-GFEM*, and therefore the $GFEM^{\mathrm{gl}}$ can be applied to problems with limited *a priori* knowledge about the solution like those involving 3-D complex fractures, multiscale or non-linear phenomena. In this method, the patch or cloud approximation spaces are built with the aid of local boundary value problems defined in a neighborhood Ω_L of a crack or other local feature of interest. Global-local enrichment functions can be built for many classes of problems. Here we report on the formulation developed for propagating three-dimensional fractures. Further details can be found in [12].

Let $\boldsymbol{u}_G^k$ denote a generalized FEM approximation of the problem at crack evolution step k. This approximation is the solution of the following problem

Find $\boldsymbol{u}_G^k \in \boldsymbol{S}_G^{GFEM,k}(\Omega) \subset H^1(\Omega)$ such that, $\forall\, \boldsymbol{v}_G^k \in \boldsymbol{S}_G^{GFEM,k}(\Omega)$

$$\int_\Omega \boldsymbol{\sigma}(\boldsymbol{u}_G^k) : \boldsymbol{\varepsilon}(\boldsymbol{v}_G^k) d\boldsymbol{x} = \int_{\partial\Omega^\sigma} \bar{\boldsymbol{t}} \cdot \boldsymbol{v}_G^k d\boldsymbol{s} \tag{1}$$

where $\boldsymbol{S}_G^{GFEM,k}(\Omega) \subset H^1(\Omega)$ is the generalized FEM space at simulation step k. The enrichment functions in $\boldsymbol{S}_G^{GFEM,k}(\Omega)$ are defined in cloud spaces and have to be computed as describe below. The mesh used to solve problem (1) is typically a *coarse* quasi-uniform mesh, *regardless of the presence of cracks in the domain*.

Fine-Scale Problem at Simulation Step k

Having the global approximation $\boldsymbol{u}_G^k$ at simulation step k, the following fine-scale problem on $\Omega_L \subset \Omega$ is solved to find enrichment functions for the space $\boldsymbol{S}_G^{GFEM,k+1}(\Omega)$:

Find $\boldsymbol{u}_L^k \in \boldsymbol{S}_L^{GFEM,k}(\Omega_L^k) \subset H^1(\Omega_L^k)$, such that $\forall\, \boldsymbol{v}_L^k \in \boldsymbol{S}_L^{GFEM,k}(\Omega_L^k)$

$$\int_{\Omega_L^k} \boldsymbol{\sigma}(\boldsymbol{u}_L^k) : \boldsymbol{\varepsilon}(\boldsymbol{v}_L^k) d\boldsymbol{x} + \kappa \int_{\partial\Omega_L^k \setminus (\partial\Omega_L^k \cap \partial\Omega)} \boldsymbol{u}_L^k \cdot \boldsymbol{v}_L^k ds = \int_{\partial\Omega_L^k \cap \partial\Omega^\sigma} \bar{\boldsymbol{t}} \cdot \boldsymbol{v}_L^k ds + \kappa \int_{\partial\Omega_L^k \setminus (\partial\Omega_L^k \cap \partial\Omega)} \boldsymbol{u}_G^k \cdot \boldsymbol{v}_L^k ds \tag{2}$$

where $\boldsymbol{S}_L^{GFEM,k}(\Omega_L^k)$ is a discretization of $H^1(\Omega_L^k)$ using the GFEM shape functions presented in [PDGJ09, pp. 10–12]. A key aspect of problem (2) is the use of the coarse-scale solution at simulation step k, $\boldsymbol{u}_G^k$, as boundary condition on $\partial\Omega_L^k \setminus (\partial\Omega_L^k \cap \partial\Omega)$. Exact boundary conditions are prescribed elsewhere on $\partial\Omega_L^k$.

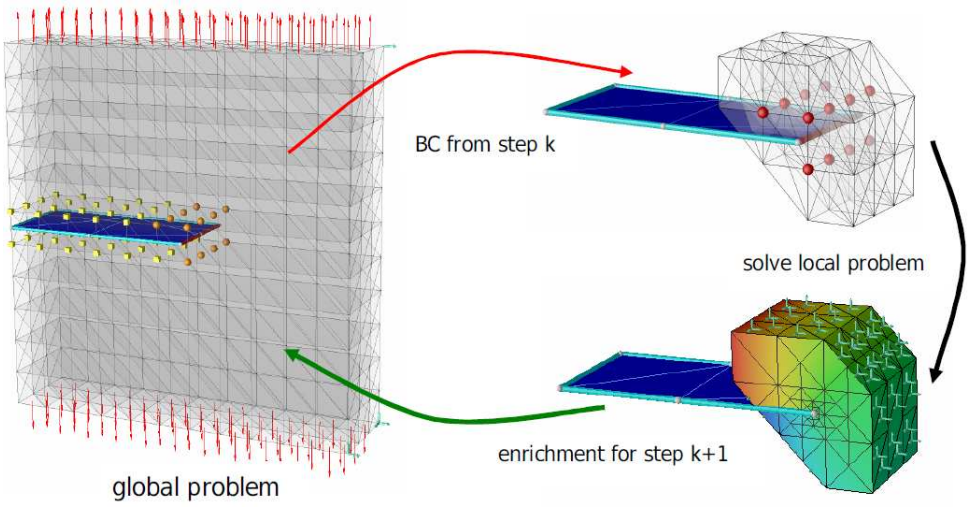

Figure 1: Model problem used to illustrate the main ideas of the *GFEM*$^{\text{gl}}$ for propagating cracks. The solution computed on the coarse global mesh provides boundary conditions for the extracted local domain in a neighborhood of the crack. *The crack is shown in the global domain for illustration purposes only*. In the *GFEM*$^{\text{gl}}$, fine-scale features are *not* discretized in the global problem. Instead, global-local enrichment functions are used [12].

Scale-Bridging with Global-Local Enrichment Functions

The solution, $\boldsymbol{u}_L^k$, of the fine-scale problem (2) is used to build generalized FEM shape functions defined on the coarse-scale (global) mesh:

$$\boldsymbol{\phi}_{\alpha i}^{k+1}(\boldsymbol{x}) := \varphi_\alpha(\boldsymbol{x})\boldsymbol{u}_L^k(\boldsymbol{x}) \tag{3}$$

where the partition of unity function, φ_α, is provided by a global, *coarse*, FE mesh and $\boldsymbol{u}_L^k$ has the role of an enrichment or basis function for the patch or cloud space $\chi_\alpha(\omega_\alpha)$. Hereafter, $\boldsymbol{u}_L^k$ is denoted a *global-local enrichment function*. The global GFEM space containing shape functions $\boldsymbol{\phi}_{\alpha i}^{k+1}$ is denoted $\boldsymbol{S}_G^{GFEM,k+1}(\Omega)$. The coarse-scale problem (1) is solved for $\boldsymbol{u}_G^{k+1} \in \boldsymbol{S}_G^{GFEM,k+1}(\Omega)$ and the procedure is repeated at each crack evolution step.

The methodology is illustrated in Figure 1. The global solution provides boundary conditions for fine-scale problems while their solutions are used as enrichment functions for the coarse-scale problem through the partition of unity framework of the GFEM.

A-Priori Error Estimate for Global-Local Enrichments

The boundary conditions applied to the local problems described above are not exact. Hence, the effect of these boundary conditions on the performance of the *GFEM*$^{\text{gl}}$ was one of the major focuses of this project. An a-priori error estimate for the local solutions was derived. Based on this estimate, two strategies to control the effect of inexact boundary conditions on the *GFEM*$^{\text{gl}}$ were developed. A summary of the main results is presented below. Details can be found in [7].

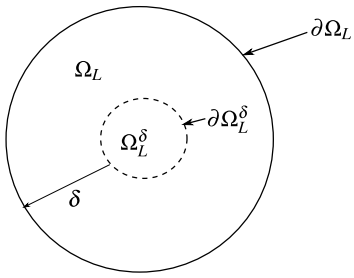

Figure 2: Local domain Ω_L and subdomain Ω_L^δ.

Let Ω_L denote the domain of a local problem and Ω_L^δ a subdomain of Ω_L such that $dist(\partial\Omega_L, \partial\Omega_L^\delta) \geq \delta > 0$ (cf. Figure 2). Parameter δ is termed as the size of a *buffer zone*. Let $\boldsymbol{u}^{exBC}$ and $\boldsymbol{u}^{inexBC}$ be the solutions of a local problem with exact and inexact boundary conditions, respectively, and $\boldsymbol{u}_h^{inexBC}$ the generalized or finite element approximation of $\boldsymbol{u}^{inexBC}$. The error $\boldsymbol{u}^{exBC} - \boldsymbol{u}_h^{inexBC}$ in the energy norm on Ω_L^δ is bounded by

$$\|\boldsymbol{u}^{exBC} - \boldsymbol{u}_h^{inexBC}\|_{\varepsilon(\Omega_L^\delta)} \leq C \inf_{\boldsymbol{x} \in \boldsymbol{X}_L^{hp}(\Omega_L)} \|\boldsymbol{u}^{inexBC} - \boldsymbol{x}\|_{\varepsilon(\Omega_L)} + \frac{C_1}{\delta} \|\boldsymbol{u}^{exBC} - \boldsymbol{u}^{inexBC}\|_{L^2(\Omega_L)} \quad (4)$$

where $\boldsymbol{X}_L^{hp}(\Omega_L)$ is a discretization of $\left(H^1(\Omega_L)\right)^3$ using GFEM or FE shape functions. The first term on the right hand side of (4) denotes the finite element discretization error, which can be controlled by refining the local mesh. The second term measures the effect of the inexact boundary conditions on the local problem boundary $\partial\Omega_L$. The estimate shows that *this term can be reduced by increasing the size of the buffer zone* δ. Furthermore, the effect of inexact boundary conditions is measured in the L^2 norm which is weaker than the energy norm.

In [7], we propose two strategies to control the error of the *GFEM*$^{\text{gl}}$ solution due to inexact boundary conditions on local problems. The first one is based on the use of a *buffer* zone as described above. The second strategy investigated is based on a computationally efficient global-local iterative process (Figure 3), wherein the solution of the enriched global problem is used again as the boundary conditions for the local problem and the process is repeated until the desired accuracy is achieved. Several numerical experiments performed on three-dimensional fracture mechanics problems illustrate the effectiveness of these strategies in controlling the error of the *GFEM*$^{\text{gl}}$ solution. The problems were selected such that the boundary conditions on the local problems ranged from smooth to singular functions. Here, we report on a representative case to illustrate the effectiveness of these approaches. The results shown in Figure 5 are obtained from simulations run on a 30" $\times$ 30" $\times$ 1" edge-crack panel with different sizes of the local domain, providing different number of layers of elements in the buffer zone. These results agree with the error estimate (4) in the sense that the effect of inexact boundary conditions decay as the size of the buffer zone increases. An important point to observe from Figure 5 is that a couple of iterations in the problems with buffer zone sizes *0-2* delivers the same error level as obtained with one iteration in the

problem with a 4 layer buffer zone. This shows that similar error levels can be obtained by either of the strategies, i.e. by multiple global-local iterations or by the use of a buffer zone.

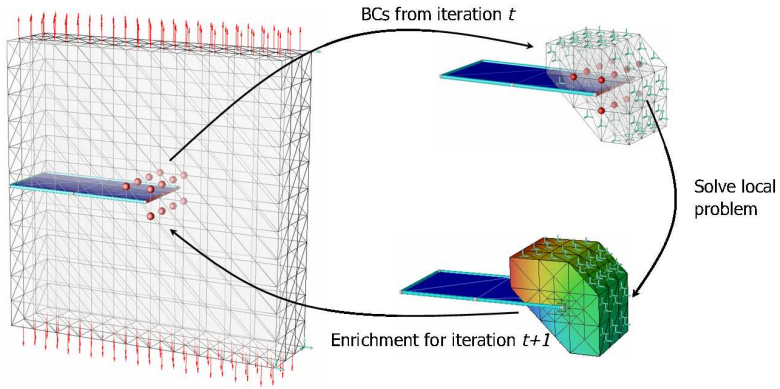

Figure 3: Illustration of the process of multiple global-local iterations to improve the quality of boundary conditions applied to a local problem around a crack front.

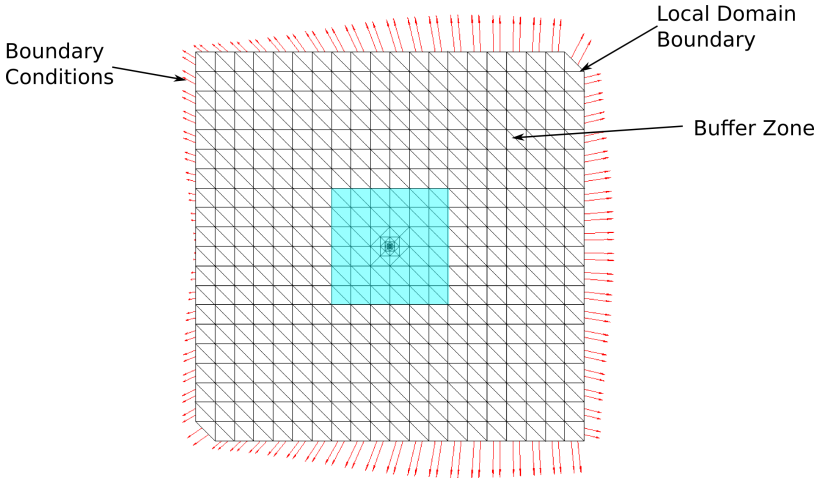

Figure 4: Buffer zone in a local domain. The blue shaded area represents the region from which the solution of local problem is used as enrichment in the enriched global problem.

Size of the Enrichment Zone

In the context of the $GFEM^{gl}$, an enrichment zone is the geometric zone (or region) of the global problem domain within which the solution of the local problem is used to enrich the global solution space with the global-local enrichment functions. In this project we have derived an estimate for the optimal size of the enrichment zone, d

$$d \geq C(h)^{\frac{1}{2p}} \tag{5}$$

where, C is a constant, h is the size of a representative finite element in the global mesh and p is the corresponding polynomial order. The proof of (5) and numerical verification of the

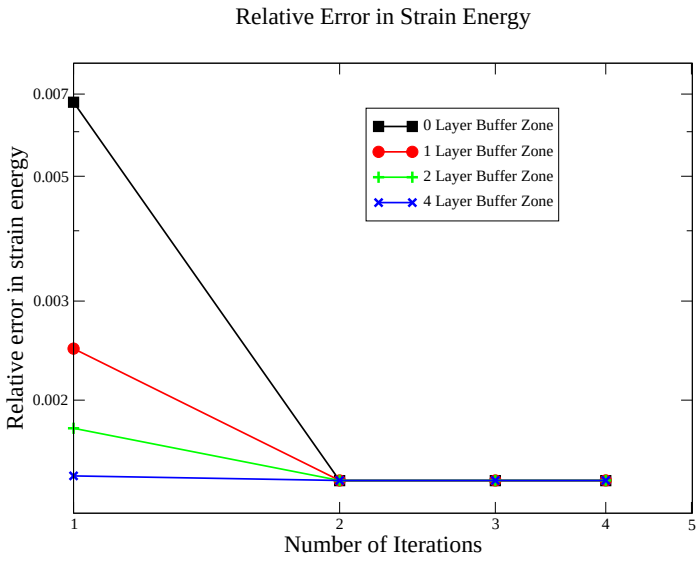

Figure 5: Relative error in Strain Energy of enriched global problem, computed with exact strain energy as the reference value, against the number of iterations, for different sizes of the buffer zone.

same through several numerical examples are given in [9].

Crack Propagation using *GFEM*^{gl}

Figure 6 shows several steps of a crack propagation simulation using an adaptive GFEM and the *GFEM*^{gl} developed in this project. Both methods predict the same crack surface path, however, there is a dramatic difference in the required mesh density and problem size in each methodology.

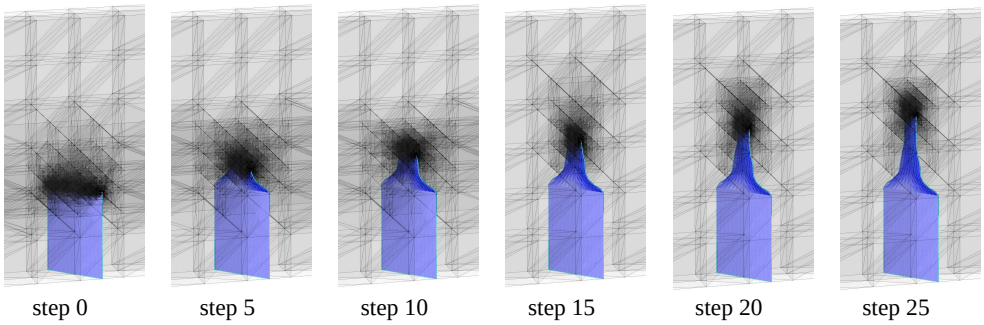

(a) *hp*-GFEM or *hp*-FEM with remeshing

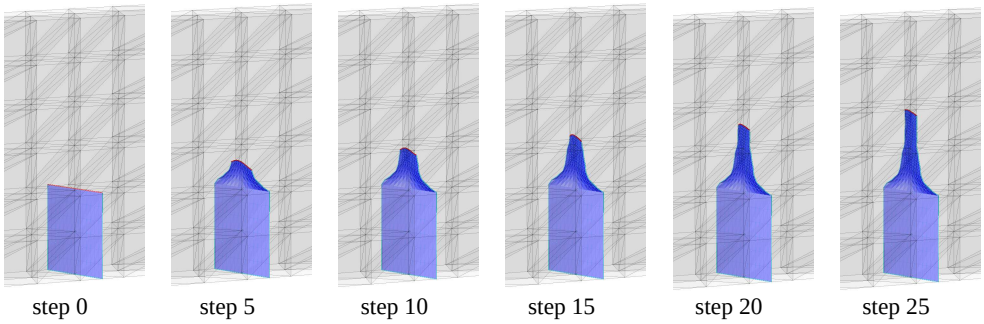

(b) *GFEM*^{gl} uses a coarse mesh enriched with global-local functions

Figure 6: Crack surface evolution and mesh for various crack steps in *hp-GFEM* and *GFEM*^{gl} simulations.

These results are published in [12].

Parallel Computation of Global-Local Enrichment Functions

A single local problem around a crack was considered in the *GFEM*^{gl} described above. While this facilitates the computational implementation of the method, it does not have to be the case. Each cloud from the global mesh can be used to define a small local problem. This procedure is illustrated in Figure 7. The creation of a large number of small local problems in the neighborhood of, e.g., a crack, instead of a single large one, is attractive since the solution of these problems lends itself to a parallel implementation. This section reports on the computational performance of a parallel implementation of the *GFEM*^{gl}. Several local problems are defined around crack fronts and solved using a single pair of scatter-gather communications. No communication amongst threads solving local problems is required.

Typical parallel FEM implementations partition the computational domain and distributes the partitions among threads such that each one processes the same computational load [Far88] However, FEM discretizations with non-uniform element sizes and/or polynomial orders are difficult to partition since estimating the computational load of each partition is not trivial [OPS92]. In the parallel implementation of the *GFEM*^{gl} developed in this project, load balancing is addressed by defining a larger number of local problems than the number of parallel threads, and by sorting and solving the local problems based on simple estimates of their workload.

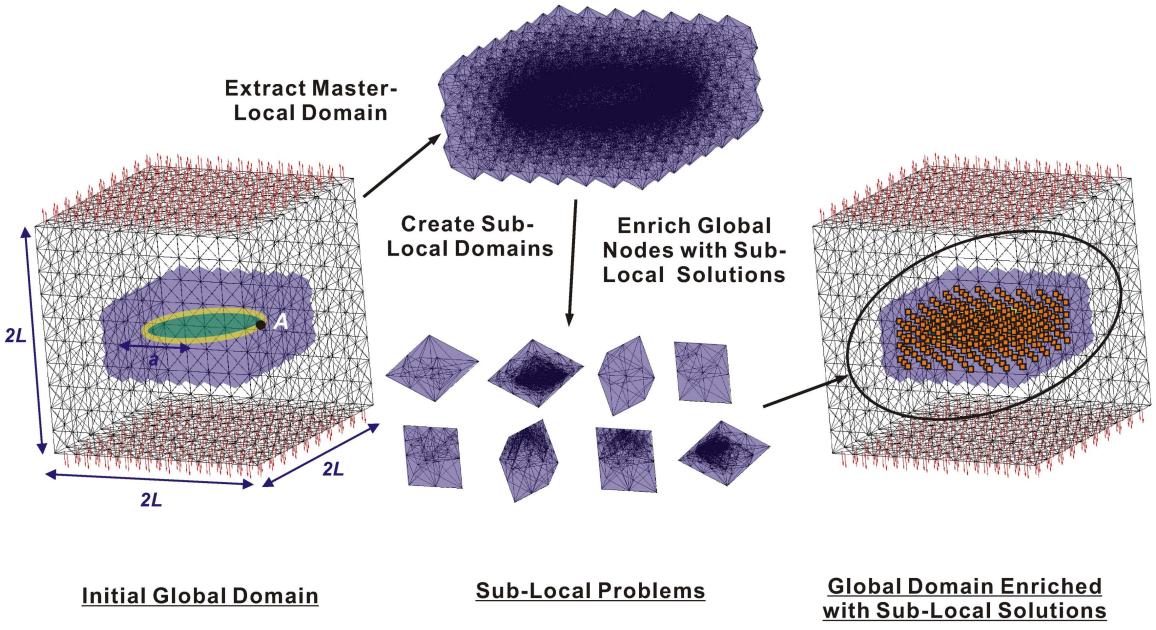

Figure 7: Illustration of parallel computation of global-local enrichment functions. Several local problems used for the computation of global-local enrichments are created around the crack front. Each local problem is sent to a different processor and efficiently solved in parallel.

The effectiveness of the proposed parallel *GFEM*^{gl} was verified through several numerical examples with the emphasis on the parallel efficiency and accuracy of the method. Here, we

report on a representative case. These results are presented in journal paper [11]. This paper appeared in the **List of Top Five Most Downloaded Papers** of *Computational Mechanics*.

Table 1 reports the parallel efficiency of the method on a representative three-dimensional problem with complex geometry. The table lists the CPU time required to solve the sub-local problems, the parallel efficiency and the speed-up with respect to the number of CPUs. It can be observed that a high parallel efficiency is attained and that the CPU time reduces from 1537 seconds to just 66.4 seconds when 32 processors are used.

Table 1: Parallel performance of *GFEM*^{gl}.

Number of CPUs	CPU time (sec.)	Parallel efficiency	Speed-up
1	1537.4	N/A	N/A
2	778.1	0.99	1.98
4	392.1	0.98	3.92
8	198.3	0.97	7.75
16	101.1	0.95	15.21
18	92.3	0.93	16.67
20	86.3	0.89	17.82
32	66.4	0.72	23.16

GFEM^{gl} for Confined Plasticity Problems

The *GFEM*^{gl} was extended in this project to problems with localized nonlinear behavior. The procedure involves the solution of boundary value problems around local regions exhibiting nonlinear behavior and the enrichment of the global solution space with local solutions through the partition of unity framework used in the generalized finite element method. The formulation and other details are given in [10]. This paper appeared in the **List of Top Five Most Downloaded Papers** of *Computational Mechanics*.

The *GFEM*^{gl} developed in this project can produce accurate nonlinear solutions with a reduced computational cost compared with standard finite element methods since computationally intensive nonlinear iterations can be performed on coarse global meshes after the creation of enrichment functions properly describing local nonlinear behavior. The effectiveness of the method was investigated in terms of accuracy and computational cost through several three-dimensional examples exhibiting confined plasticity. A representative example from [10] is presented here.

Figure 8 describes this *GFEM*^{gl} procedure to analyze an L-shaped domain subjected to constant vertical tractions. The local domain is created around the re-entrant corner of the domain where plastic strains are concentrated.

Figure 9 shows the von Mises stress distributions obtained from the *hp-GFEM* (Direct Numerical Simulation) and the *GFEM*^{gl}. The quality of the *GFEM*^{gl} solution is comparable

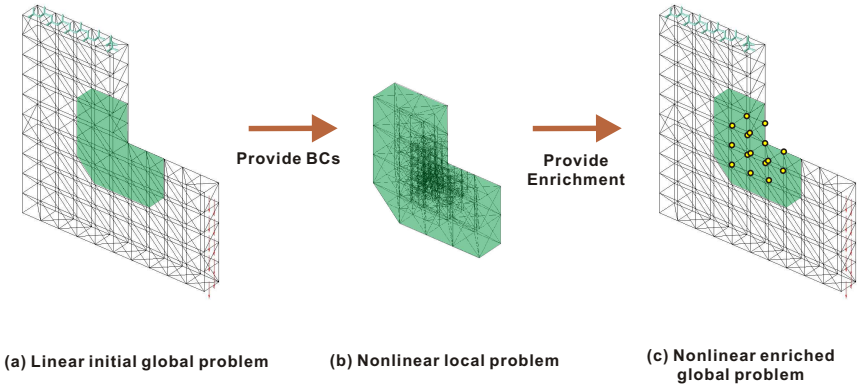

Figure 8: Nonlinear solution procedure for the L-shaped domain example using the *GFEM*$^{\text{gl}}$ developed in this project.

to or even better than that of the *hp-GFEM* solution even though a coarse global mesh is used for the *GFEM*$^{\text{gl}}$ analysis [10].

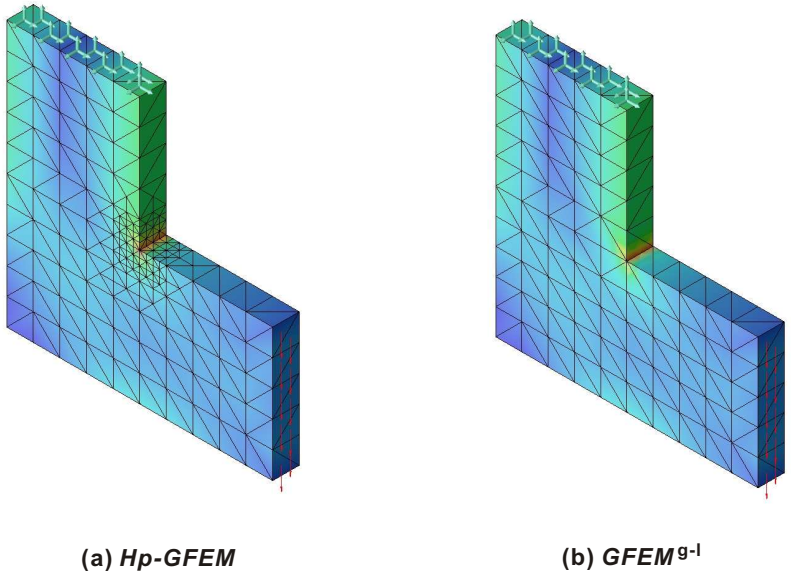

Figure 9: Von Mises stress distributions in the L-shaped domain example computed by the *hp-GFEM* and *GFEM*$^{\text{gl}}$. The new *GFEM*$^{\text{gl}}$ for non-linear problems is able to capture highly localized non-linear responses using coarse meshes at the structural scale.

GFEM$^{\text{gl}}$ for Nonlinear Fracture Problems

The formulation proposed in [10] was extended to three-dimensional fracture problems involving confined plasticity. The results from this study are published in [8], an illustrative example from which is shown in Figure 10. It is an edge-crack panel subjected to uniform tractions of magnitude $t_y = 12.50$ on the top and bottom faces. The thickness of the panel in the z-direction is unity. This figure also shows the global finite element mesh, a uniform

mesh of tetrahedron elements, used to solve the problem, along with the traction boundary conditions.

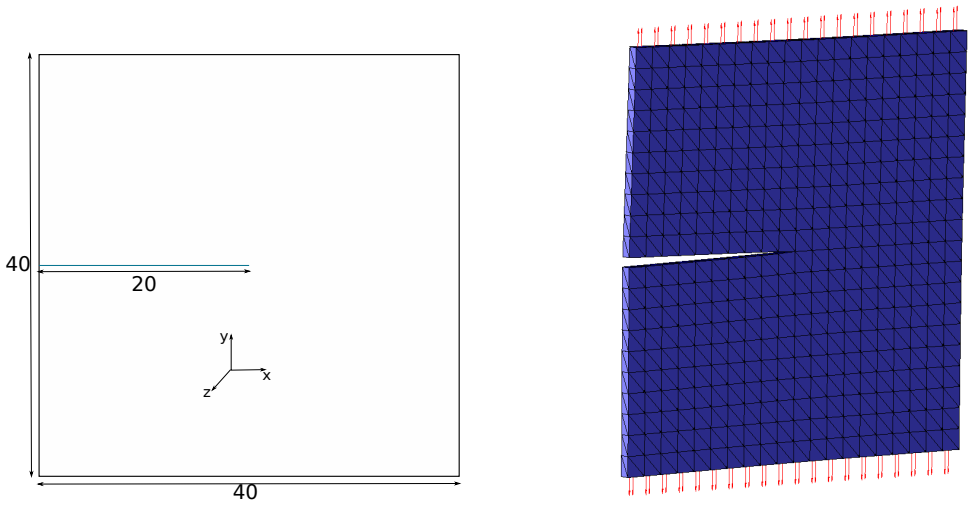

Figure 10: Three-dimensional edge-crack panel subjected to uniform tractions on the top and bottom faces. The right figure features the global finite element mesh with the applied tractions.

The procedure to analyze this problem using the *GFEM*$^{\text{gl}}$ is illustrated in Figure 11. The first step in this procedure involves the solution of the global problem on a coarse mesh with the full load applied and assuming a linear elastic material model. A local domain, which fully contains the region with plastic deformations, is then automatically extracted from this coarse global mesh as shown in the figure. The solution of the initial global problem, obtained in the first step is used to prescribe boundary conditions for the local problem. The local problem is solved nonlinearly using Newton-Raphson iterations. The computed nonlinear local solution at the final load step is then used to enrich the global solution space at certain nodes in the coarse global mesh (shown as red spheres in Figure 11). This *enriched global problem* is then solved nonlinearly using Newton-Raphson iterations. Figures 12 and 13 show the contour plots of the distribution of the equivalent plastic strain obtained with the *GFEM*$^{\text{gl}}$ and *hp-GFEM*, respectively. As can be seen from the figures, the plastic strain distribution in the two cases are very similar, in spite of using a coarse global mesh in the case of *GFEM*$^{\text{gl}}$. Figure 14 shows the deformed shape of the edge-crack panel obtained in the case of *GFEM*$^{\text{gl}}$. This figure clearly shows the blunting ahead of the crack front due to plastic deformations.

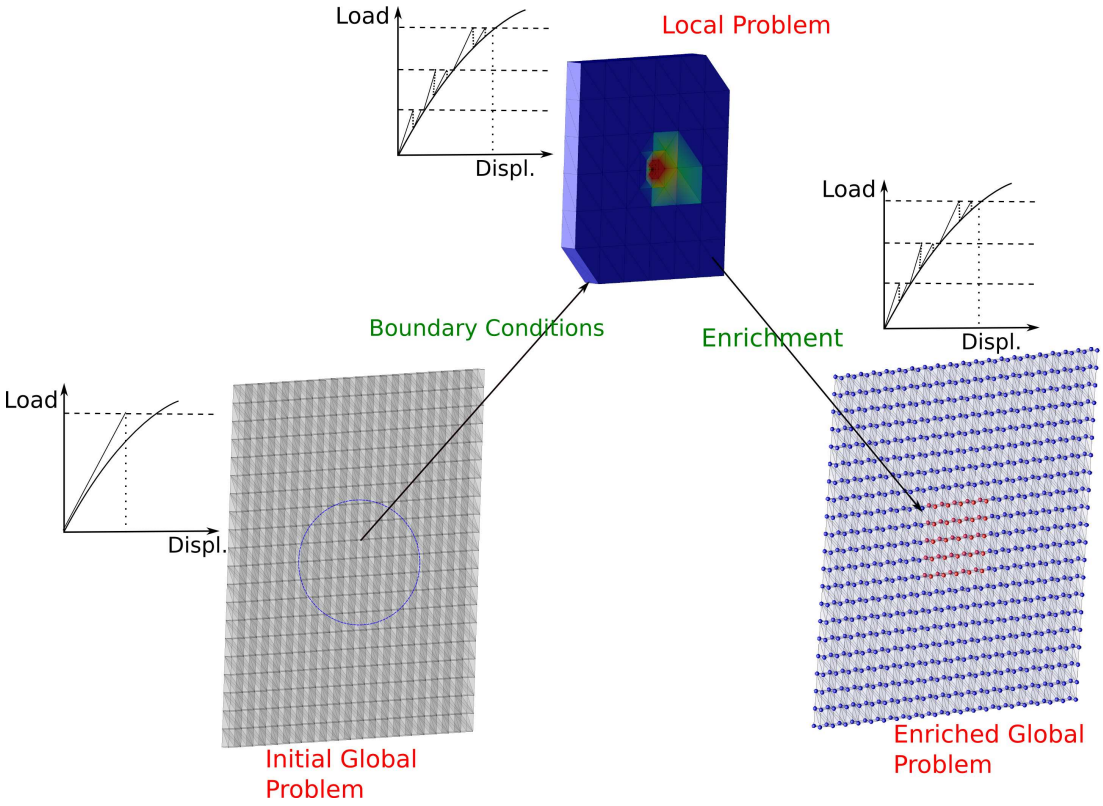

Figure 11: Figure showing the algorithm for the nonlinear solution of the edge-crack panel problem using the *GFEM*^{gl}. Red nodes in the enriched global problem indicate nodes with global-local enrichments.

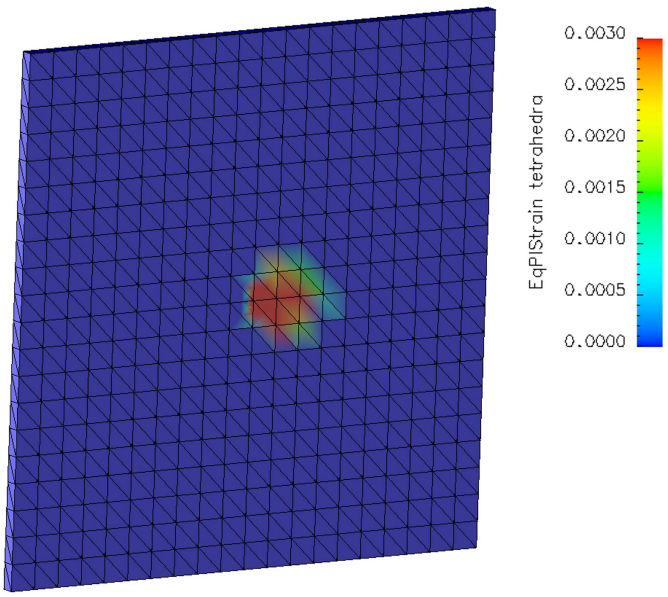

Figure 12: Figure showing the distribution of equivalent plastic strain in the case of *GFEM*^{gl}.

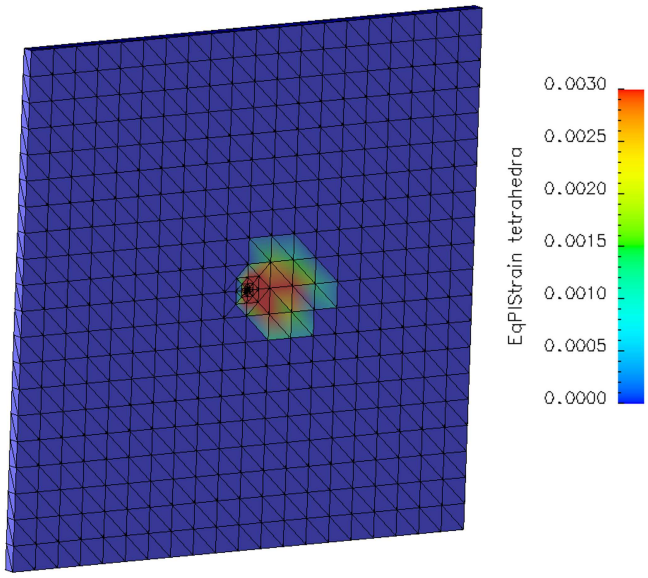

Figure 13: Figure showing the distribution of equivalent plastic strain in the case of the *hp-GFEM*.

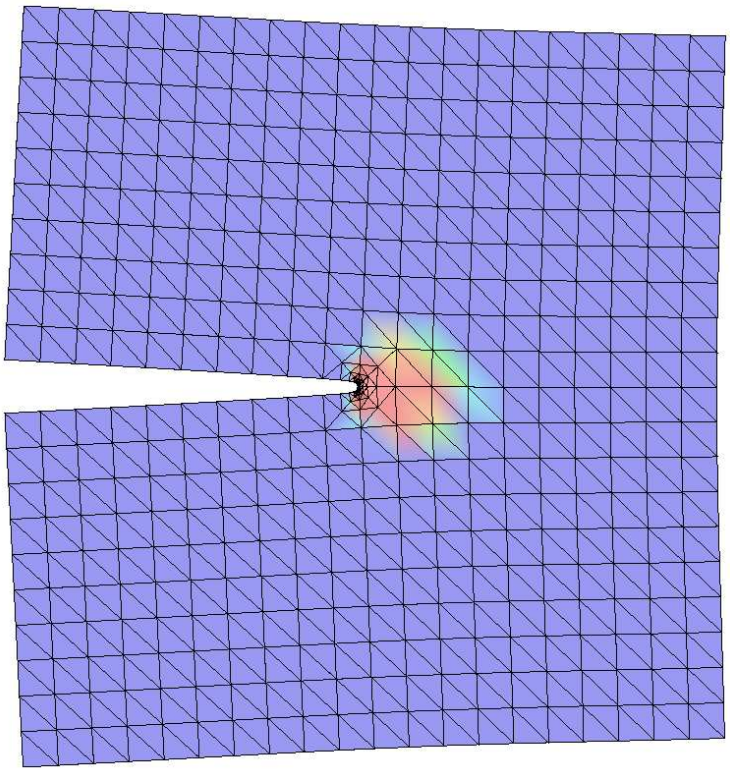

Figure 14: Figure showing the deformed configuration (scaled by a factor of ten) of the edge-crack panel in the case of the $GFEM^{gl}$. Note that the refined mesh close to the crack front correspond to graphical elements used for visualization. The computations are performed on the coarse mesh shown in Figure 12

.

Stable *GFEM*

The *GFEM* allows great freedom in the selection of enrichment functions. Babuška and Banerjee [BB12] have recently proposed modifications to available enrichments for the *GFEM* in order to create functions that are near orthogonal. They have shown that the conditioning of this so-called Stable *GFEM* (*SGFEM*) is not worse than that of the standard FEM. Moreover, their modified enrichment functions lead to optimal convergence rates at finite elements that are only partially enriched, the so-called blending elements [BMMB05]. During the past year, we worked on extensions of *SGFEM* in collaboration with Prof. Ivo Babuška from University of Texas at Austin and Prof. Uday Banerjee from Syracuse University. This collaboration is at no cost to the U.S. Air Force.

Let φ_α , $\alpha = 1,...,N$, denote Lagrangian finite element shape functions, i.e., a partition of unity. Let $L_{\alpha i}$ denote an enrichment function. The modified enrichment function, $\bar{L}_{\alpha i}$, is given by

$$\bar{L}_{\alpha i} = L_{\alpha i} - \mathscr{I}_{\omega\alpha}(L_{\alpha i}) \tag{6}$$

where $\mathscr{I}_{\omega\alpha}(L_{\alpha i})$ is an interpolation of $L_{\alpha i}$ on the patch ω_α . This interpolation is defined using the partition of unity [BB12]. The following problem provides a representative example to compare the *GFEM* and *SGFEM* approach:

- Domain: $[0,1]\times[0,1]$
- Crack: $(0,1/2)$ to $(1/2,1/2)$.
- Mesh: uniform, $h = \frac{1}{32}$.
- Crack matches with the mesh; crack-tip is on a node.
- Manufactured solution: $\mathbf{u}_I(r,\theta) = \sqrt{r}\mathbf{f}(\theta)$; $-\pi < \theta < \pi$; $\mathbf{f}(\theta)$ is discontinuous at the crack-line

$$\mathbf{u}_I(r,\theta) = \sqrt{r}\left\{\begin{array}{l}\left(\kappa-\frac{1}{2}\right)\cos\frac{\theta}{2}-\frac{1}{2}\cos\frac{3\theta}{2}\\ \left(\kappa+\frac{1}{2}\right)\sin\frac{\theta}{2}-\frac{1}{2}\sin\frac{3\theta}{2}\end{array}\right\} \tag{7}$$

where r and θ are polar coordinates at the crack tip and $-\pi \le \theta \le \pi$, κ is a material constant $(3-4\nu)$, and ν is the Poisson's ratio.

- Enrichment region: $[0,\frac{1}{2}+d]\times[\frac{1}{2}-d,\frac{1}{2}+d]$, $d = 1/8$.
- Enrichment: exact, i.e., $\mathbf{u}_I(r,\theta) = \sqrt{r}\mathbf{f}(\theta)$ at all the nodes in the enrichment region.

In the computations, nodes shown in red are enriched with functions (7) *and* the first term of the Mode II expansion, namely

$$\mathbf{u}_{II}(r,\theta) = \sqrt{r}\left\{\begin{array}{l}\left(\kappa+\frac{3}{2}\right)\sin\frac{\theta}{2}+\frac{1}{2}\sin\frac{3\theta}{2}\\ \left(\kappa-\frac{3}{2}\right)\cos\frac{\theta}{2}+\frac{1}{2}\cos\frac{3\theta}{2}\end{array}\right\} \tag{8}$$

Figures 15 and 16 show the contour plots for the distribution of element-wise error in energy norm obtained in the cases of *GFEM* and *SGFEM* respectively. Note that the red nodes in these figures are enriched with the singular functions defined by equations (7) and (8). The much reduced error levels in case of *SGFEM* can be clearly seen from these

figures, even in the interior of the enrichment region. Table 2 shows the relative error in energy norm and the condition number of the resulting stiffness matrix in the two cases. The relative error in energy norm obtained with *SGFEM* is almost half as that obtained in the case of *GFEM*. The *SGFEM* also shows an improvement in the Condition Number which would become much more significant for larger problems.

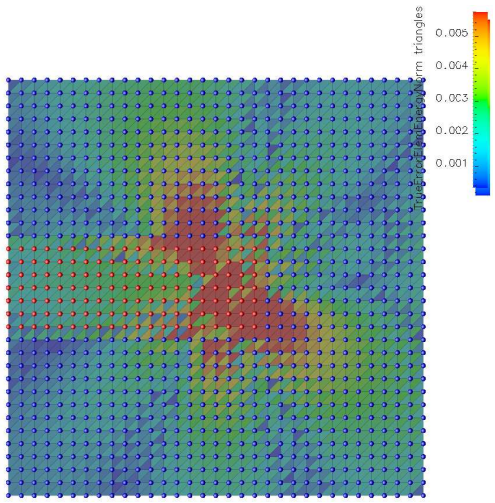

Figure 15: Contour plot for element-wise error in energy-norm obtained with *GFEM*. Red nodes are enriched with the singular functions defined by equations (7) and (8).

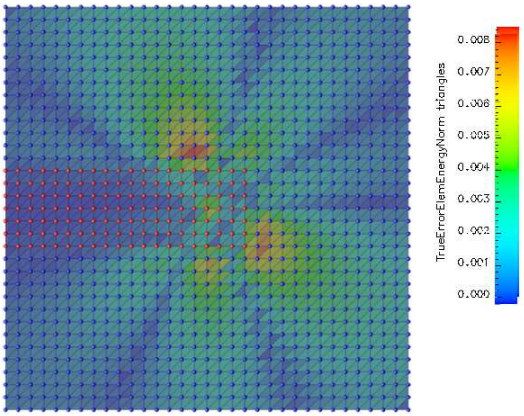

Figure 16: Contour plot for element-wise error in energy-norm obtained with *SGFEM*. Red nodes are enriched with the singular functions defined by equations (7) and (8).

	GFEM	*SGFEM*
Relative Error in Energy Norm	0.106202703	0.052492384
Condition Number	$8.49689329903 \times 10^5$	4.6211911755×10^4

Table 2: Table showing relative error in energy norm and condition number for *GFEM* and *SGFEM*

Acknowledgment/Disclaimer This work was sponsored in part by the Air Force Office of Scientific Research, USAF, under grant/contract number FA9550-09-1-0401. The views and conclusions contained herein are those of the author and should not be interpreted as necessarily representing the official policies or endorsements, either expressed or implied, of the Air Force Office of Scientific Research or the U.S. Government.

Personnel Supported by Grant

Dae-Jin Kim (May/15 – Jun/30 2009), Graduate Student, University of Illinois at Urbana-Champaign
Varun Gupta (May 15 2009 – February 2012), Graduate Student, University of Illinois at Urbana-Champaign
C. Armando Duarte, Associate Professor, University of Illinois at Urbana-Champaign

References

[BB12] I. Babuka and U. Banerjee. Stable generalized finite element method (sgfem). *Computer Methods in Applied Mechanics and Engineering*, 201204(0):91 – 111, 2012.

[BMMB05] E. Béchet, H. Minnebo, N. Moës, and B. Burgardt. Improved implementation and robustness study of the x-fem for stress analysis around cracks. *International Journal for Numerical Methods in Engineering*, 64:1033–1056, 2005.

[Far88] C. Farhat. A simple and efficient automatic fem domain decomposer. *Computers and Structures*, 28:579–602, 1988.

[OPS92] J. T. Oden, A. Patra, and Feng. Y. S. An *hp* adaptive strategy. In A. K. Noor, editor, *Adaptive, Multilevel and Hierarchical Computational Strategies*, pages 23–46. ASME, 1992. AMD-Vol. 157.

[PDGJ09] J.P. Pereira, C.A. Duarte, D. Guoy, and X. Jiao. *Hp*-Generalized FEM and crack surface representation for non-planar 3-D cracks. *International Journal for Numerical Methods in Engineering*, 77(5):601–633, 2009.

Publications and Presentations

[1] C.A. Duarte. Bridging scales with a generalized finite element method. In *Eleventh US National Congress on Computational Mechanics*, Minneapolis, MN, USA, July 2011. **Invited Keynote Presentation**.

[2] C.A. Duarte. Bridging scales with a generalized finite element method. In *IUTAM Symposium on Linking Scales in Computations: from Microstructure to Macro-scale Properties*, Pensacola, FL, USA, May 17-19 2011. **Keynote Lecture**.

[3] C.A. Duarte. Bridging scales with a generalized finite element method. In *EC-COMAS Thematic Conference on Extended Finite Element Methods-XFEM 2011*, Cardiff, United Kingdom, June 29-July 1 2011. **Plenary Lecture**.

[4] C.A. Duarte, J.P. Pereira, and D.-J. Kim. Analysis of three-dimensional propagating cracks: A two-scale approach using coarse finite element meshes. In *IV European Conference on Computational Mechanics –ECCM 2010*, May 2010. **Invited Keynote Presentation**.

[5] J. Garzon, V. Gupta, A. Simone, and C.A. Duarte. Bridging scales with a generalized finite element method. In *IUTAM Symposium on Linking Scales in Computations: From Microstructure to Macro-scale Properties*, volume 3, pages 162 – 181, 2012.

[6] V. Gupta, D.-J. Kim, and C.A. Duarte. On the robustness of the generalized finite element method with global-local enrichments. In *Eleventh US National Congress on Computational Mechanics*, Minneapolis, MN, USA, July 2011.

[7] V. Gupta, D.-J. Kim, and C.A. Duarte. Analysis and improvements of global-local enrichments for the generalized finite element method. *Computer Methods in Applied Mechanics and Engineering*, 2012. Accepted for publication.

[8] V. Gupta, D.-J. Kim, and C.A. Duarte. Extensions of the two-scale generalized finite element method to nonlinear fracture problems. *International Journal for Multiscale Computational Engineering*, 2012. Submitted.

[9] V. Gupta, D.-J. Kim, and C.A. Duarte. On the enrichment zone for generalized finite element method, 2012. To be submitted.

[10] D.-J. Kim, C. Duarte, and S. Proenca. A generalized finite element method with global-local enrichment functions for confined plasticity problems. *Computational Mechanics*, pages 1–16, 2012. Appeared in the **List of Top Five Most Downloaded Papers**.

[11] D.-J. Kim, C.A. Duarte, and N.A. Sobh. Parallel simulations of three-dimensional cracks using the generalized finite element method. *Computational Mechanics*, 47(3):265–282, 2011. Appeared in the **List of Top Five Most Downloaded Papers**.

[12] J.P. Pereira, D.-J. Kim, and C.A. Duarte. A two-scale approach for the analysis of propagating three-dimensional fractures. *Computational Mechanics*, 49(1):99–121, 2012.

AFRL Point of Contact

Dr. Thomas Eason, AFRL, Air Vehicles Directorate, WPAFB, OH, Phone 937-255-3240, e-mail Thomas.Eason@wpafb.af.mil

Transitions

1. The parallel algorithms for the computation of global-local enrichments developed in this research effort are being used by the group of Dr. Thomas Eason.

2. The *GFEM*^{gl} developed in this project is fully compatible with the standard FEM. This, together with the hierarchical nature of the global-local enrichments, allow adding the method as an external module to existing FEM codes. This feature of the method was the subject of an AFRL project aimed at a non-intrusive implementation of the *GFEM*^{gl} in a commercial FEM. The co-PI of this project was Dr. Thomas Eason.

Impact in the Research Community

The research results of this project has attracted considerable attention from the computational mathematics research community. The first evidence of this impact is the various keynote and plenary lecture invitations received by the P.I. The second evidence is that publications [10] and [11] appeared in the **List of Top Five Most Downloaded Papers** of *Computational Mechanics*.